The Mechanism of Increased Intestinal Palmitic Acids Absorption and The Impact On Hepatic Stellate Cell Activation in Non-Alcoholic Steatohepatitis

Masakazu Hanayama
Ehime University
Yasunori Yamamoto
Ehime University
Hiroki Utsunomiya
Ehime University
Osamu Yoshida
Ehime University
Liu Shuang
Ehime University
Masaki Mogi
Ehime University
Bunzo Matsuura
Ehime University
Eiji Takeshita
Ehime University
Yoshiou Ikeda
Ehime University
Yoichi Hiasa (hiasa@m.ehime-u.ac.jp)
Ehime University

Research Article

Keywords: Dietary palmitic acids, non-alcoholic fatty liver, NASH

Posted Date: February 8th, 2021

DOI: https://doi.org/10.21203/rs.3.rs-156446/v1

Abstract

Dietary palmitic acids (PAs) promote liver fibrosis in patients with non-alcoholic steatohepatitis (NASH). This study aimed to clarify the intestinal absorption kinetics of dietary PAs and the effect of trans-portal PAs on the activation of hepatic stellate cells (HSCs) involved in liver fibrosis in patients with NASH. First, we found that the concentration of blood PAs after meals was significantly increased in NASH patients compared to control patients ($P < 0.01$). Second, gene expressions associated with fat absorption and chylomicron formation, such as CD36 and MTP, were significantly increased in the intestine of the NASH model rats fed a high-fat-cholesterol diet compared to control rats. Furthermore, portal PA levels after meals in the NASH model rats were significantly higher compared to control and non-alcoholic fatty liver (NAFL) rats ($P<0.01$). Third, PA injection via the portal vein to the liver in control rats increased the mRNA levels associated with the activation of HSCs and the expression of α-SMA in liver tissues.

Our study showed an increased intestinal absorption of dietary-derived PA in NASH. The rapid increase in PAs via the portal vein to the liver may activate HSCs and affect the development of liver fibrosis in NASH.

Introduction

Non-alcoholic fatty liver disease (NAFLD) is a chronic liver disease in which about 20% of patients develop non-alcoholic steatohepatitis (NASH) with hepatitis and fibrosis[1]. Some NASH patients develop cirrhosis and hepatocellular carcinoma with a poor prognosis, the prevalence of which is increasing worldwide. Fatty acids (FAs) play an important role in the pathogenesis of NASH. Long-chain fatty acids (LCFAs) induce lipid deposition, inflammation, and reactive oxygen species (ROS) production in the liver[2,3]. In particular, palmitic acid (PA) shows strong lipotoxicity for the liver[4,5]. Dietary FAs and intestinal chylomicrons (CMs) are one of the major sources of PAs in NASH[6,7].

Previous studies have shown that the intestinal absorption of ^{13}C-labeled palmitate was significantly higher in patients with NASH than in healthy controls, and a strong association with clinical parameters related to hepatic steatosis and fibrosis in the early stage of NASH has been reported[8]. Another study reported the increased absorption of dietary PAs in patients with cirrhosis[9]. Liver fibrosis is mediated by activated hepatic stellate cells (HSCs) during tissue repair[10]. However, the association between dietary PAs and HSCs in the pathogenesis of NASH remains unknown. We hypothesized that the overflow of dietary PA to the liver affects the HSCs in NASH.

In this study, we identified the mechanism of increased intestinal PA absorption using a NASH model rat and evaluated the effect of dietary PAs via the portal vein on the activation of HSCs in NASH.

Materials And Methods

Human subject

Experimental procedures were performed in accordance with the approved guidelines. Thirty-nine healthy subjects and 41 NASH patients were enrolled between January 2012 and August 2015. The study was performed using a protocol approved by the Institutional Review Board of Ehime University Hospital (approval number: 1407006). All enrollees in the study received informed consent, and the protocol of the study followed the guidelines of the Declaration of Helsinki.

FA analysis

All subjects received blood samples during hospitalization at the time of fasting and 2 hours after breakfast intake. Serum was collected from the blood, and serum FA concentrations were measured by gas chromatography, and the relative change in FA was calculated according to Equation 1

Relative change = FA concentration after a meal / fasting FA concentration (1)

Animals

Eight-week-old male Sprague Dawley (SD) rats (CLEA Japan, Tokyo, Japan) were maintained in a 12-hour light/dark cycle. The disease model rats were bred according to published methods[41]. Rats were randomly assigned to three groups and fed the assigned diets for 18 weeks as follows: (1) the control group fed MF normal diet (MF; Oriental Yeast, Tokyo, Japan), (2) the NAFL group fed a high-fat diet (HFD) (68% MF, 30% palm oil, 2% cholic acid), and (3) the NASH group fed a high-fat high-cholesterol diet (HFCD) (68% MF, 27.5% palm oil, 2.5% cholesterol, 2% cholic acid). Animals were allowed *ad libitum* access to water. All procedures were approved by the Ehime University Animal Care Committee. All studies were performed in compliance with ARRIVE guidelines.

Determination of lipid and FA absorption and chylomicron production

All rats fasted overnight before the procedure. Cannulas were placed in the portal vein and duodenum under isoflurane anesthesia. The rats were then infused with the lipid emulsion at a rate of 3 mL/h into the duodenum. The emulsion consisted of 12.5 μmol glycerol tripalmitate (Wako, Osaka, Japan), 57 μmol sodium taurocholate, and 7.8 μmol phosphatidylcholine in 3 mL of PBS. Triton WR-1339 (0.5 g/kg) (Tyloxapol; Sigma–Aldrich Co, St. Louis, MO, USA) was administered 20 min after beginning the emulsion infusion. Blood was collected from the portal vein every 30 min for 3 h. Plasma triglyceride (TG) levels were measured using enzymatic kits (Triglyceride E-test; Wako, Osaka, Japan). Plasma CM levels were measured using high-performance liquid chromatography (HPLC) (LipoSEARCH; Skylight Biotech, Akita, Japan). Plasma PA levels were measured using gas chromatography.

Determination of coefficient of intestinal lipid absorption

Twenty-four-hour stools were collected, and the 24-h dietary intake of meals was measured. Lipids in stool and feed were extracted using the Blight and Dyer method[42], and their respective lipid contents were determined. Lipid absorption coefficient (LAC) was calculated according to Equation 2:

$$LAC = \frac{(dietary\ lipid\ intake - lipid\ defecation)}{dietary\ lipid\ intake} \times 100 \qquad (2)$$

FA absorption after glucagon-like peptide-2 (GLP-2) administration

After overnight fasting, plasma GLP-2 concentrations were measured using a rat GLP-2 ELISA kit (Yanaihara Institute, Fujinomiya, Japan). After overnight fasting, control rats were infused with the lipid emulsion at a rate of 3 mL/h into the duodenum, and Triton WR-1339 (0.5 g/kg) with or without the GLP-2 analog (0.25 mg/kg) (Bachem, Bubendorf, Switzerland) was administered after 20 min. We collected blood from the portal vein every 30 min for 3 h and measured plasma TG levels.

Identification of genes involved in lipid and FA absorption

To analyze the expression of genes involved in lipid and FA absorption in the intestine, real-time PCR and western blot analysis were performed using jejunal tissues.

Measurement of liver fibrosis markers after portal administration of PA

PA (0.0256 μg) was added to 1,000 μL 99% ethanol to prepare solution (A). Next, 1.0 g bovine serum albumin (BSA) was mixed with 9 mL water and 40 μL 1N NaOH solution (B). We then added 100 μL solution (A) to 900 μL solution (B) to prepare the PA solution. One milliliter PA solution was administered to the portal vein of rats under anesthesia. Liver tissues were collected 24 h after the administration, and the expression of liver fibrosis markers was determined.

Real-time PCR

RNA was extracted from the jejunum and liver using a RNeasy Plus mini kit (Qiagen, Hilden, Germany). Reverse transcription reactions were performed using the high capacity cDNA reverse transcription kit (Thermo Fisher Scientific, Waltham, MA, USA). Real-time PCR was performed using the LightCycler 480II (Roche Diagnostics, Mannheim, Germany). The primer sequences used are provided in Supplementary Table 2. Gene expression data were normalized to the expression of the b-actin and expressed as a ratio of the values obtained in control rats.

Western Blotting

Rat jejunal tissue proteins were run on Mini-PROTEAN TGX 7.5% stain-free gels (Bio-Rad, California, USA) and transferred to Immuno-Blot low fluorescence polyvinylidene fluoride (PVDF) membranes. Stain-free technology (Bio-Rad) was used to determine equivalent loads. Membranes were visualized using the ChemiDoc Touch imaging system (Bio-Rad). Quantification was performed using ImageLab 5.0 software (Bio-Rad). Bands were normalized to total protein, as previously reported[43]. The following antibody was used to detect CD36: CD36 (LSBio #LS-B662).

Assessment of liver fibrosis

Liver tissues were stained with hematoxylin and eosin (H&E). The tissue was then stained with Sirius Red in picric acid to assess liver fibrosis.

Immunohistochemical staining

Formalin-fixed and paraffin-embedded rat liver tissues were used. Immunostaining was performed using polyclonal α-smooth muscle actin (α-SMA) (1:200; Thermo Scientific # RB-9010) as the primary antibody; and MAX-PO(R) (Nichirei #414181) was used as the secondary antibody. After immunostaining, the colors were developed using 3,3′-diaminobenzidine (DAB) chromogen, and the tissues were evaluated.

Statistical analysis

Results are presented as mean ± standard deviation (SD). Statistical analyses were performed using post hoc Mann–Whitney U test, unpaired Student's *t*-test, paired *t*-test, and one-way analysis of variance (ANOVA), followed by Tukey's multiple comparison test. All statistical analyses were performed using R (The R Foundation for Statistical Computing, Vienna, Austria).

Results

Serum PA levels are increased in NASH patients after meals.

The patient background is shown in supplemental Table 1. First, we measured the relative change in FA level in serum before and after meals. Only the relative change in saturated fatty acids (SFA) was significantly increased in NASH patients compared to controls ($p < 0.01$, Fig. 1A). From this result, we measured the relative change in each fraction of SFA and found that among the SFAs, only the change in PA was significantly increased ($p < 0.01$, Fig. 1B).

NASH rats exhibit liver fibrosis and HSCs activation

We performed experiments using Sprague Dawley (SD) normal rats and non-alcoholic fatty liver (NAFL) rats fed a high-fat diet (HFD) and NASH rats fed a high-fat-cholesterol diet (HFCD). First, we performed H&E staining, Sirius Red staining, and immunostaining for α-SMA in liver tissues to evaluate fat deposition and liver fibrosis in each group. We then performed RT-PCR analysis of genes related to the activation of HSCs. Fat deposits were observed in the livers of NAFL rats and NASH rats; however, the degree of fat deposition was more significant in NASH rats than in NAFL rats (Fig. 2A). Moreover, liver fibrosis was confirmed in NASH rats. Although α-SMA-positive cells were observed in both NAFL and NASH rats, more were found in the livers of NASH rats.

Next, we measured the mRNA levels of molecules involved in the activation of HSCs. In NAFL and NASH rats, the expression of *Tgfb* (TGF-β) mRNA was significantly higher than that in controls ($P < 0.01$); meanwhile, the expression in NASH rats was significantly higher than that in NAFL rats ($P < 0.01$). In the NAFL and NASH rats, the expression of *Col1A1*, *Acta2* (α-SMA), *Timp1* (TIMP-1) mRNA was significantly higher than that in controls ($P < 0.01$). The expression of *Serpine1* (PAI-1) mRNA was significantly higher

in the NASH group than in controls ($P < 0.05$) (Fig. 2B). These results show that HSCs were activated and that remarkable fibrosis occurred in the liver of NASH rats.

PA absorption increases in the intestine of NASH model rats

We administered lipid emulsion continuously to the duodenum of each model rat and monitored triglyceride (TG) concentration in portal plasma. We also administered Triton WR-1339 intravenously for blocking lipoprotein catabolism. After 180 min, the TG concentration in the portal plasma was 317.9 ± 32.2, 370.8 ± 33.7, and 419.2 ± 28.9 mg/dL for the control, NAFL, and NASH rats, respectively. TG concentration in portal plasma was significantly higher in the NASH ($P < 0.01$) and NAFL ($P < 0.05$) groups than in the control (Fig. 3A).

Next, we determined the total chylomicron (CM) particle number and the concentration of TG present in plasma CM (CM-TG) using high-performance liquid chromatography (HPLC). Total CM particle number (Fig. 3B) and concentration of CM-TG (Fig. 3C) were significantly higher in the NASH ($P < 0.01$) and NAFL ($P < 0.01$) groups compared to the control. Furthermore, the NASH group had significantly higher CM particle counts than did the NAFL group ($P < 0.05$). PA concentration in the portal vein after administration of lipid emulsion was significantly higher in NASH ($P < 0.01$) and NAFL ($P < 0.01$) rats compared to the control (Fig. 3D). Furthermore, PA concentration in the NASH group was significantly higher than that in the NAFL group ($P < 0.01$). The Lipid absorption coefficient (LAC) in the NASH ($P < 0.01$) and NAFL models ($P < 0.05$) was significantly higher than that in the control (Fig. 3E). Furthermore, the LAC in the NASH group was significantly higher than that in the NAFL group ($P < 0.01$).

Genes involved in FA absorption are highly expressed in the intestine of NASH rats

We evaluated the expression of genes that contribute to the absorption and synthesis of FA and lipids via CM (Fig. 4A)[11-18]. The expression level of *Cd36* (CD36) mRNA was significantly higher in NASH rats compared to controls ($P < 0.05$). *Mtp* (MTP) mRNA expression levels involved in CM formation were significantly higher in the NASH ($P < 0.01$) and NAFL models ($P < 0.05$) compared to the control, while Apo-B levels were significantly higher in the NASH group compared to the other two groups ($P < 0.05$). *APOA-IV* mRNA expression was significantly higher in NASH and NAFL rats than in controls ($P < 0.01$). *Fatp4* (FATP4) mRNA levels were significantly higher in NASH and NAFL rats than in controls ($P < 0.05$). Both *Fabp1* (liver fatty acid-binding protein; $P < 0.01$) and *Fabp2* (intestinal fatty acid-binding protein; $P < 0.05$) mRNA levels, which are involved in FA transport, were significantly higher in the NASH group than in the control. The mRNA expression levels of *Ern2* (inositol-requiring enzyme 1β) and *Sar1b* (Ras-related GTPase 1b), which are involved in CM formation, did not vary significantly among these groups (Fig. 4A). We then analyzed the CD36 protein level in jejunal tissues (Fig. 4B) and found that the expression of glycosylated CD36, an activated form of CD36, was significantly higher in the NASH model compared to the control.

Glucagon-like peptide-2 (GLP-2) promotes intestinal lipid absorption

The plasma GLP-2, which activates intestinal CD36 by glycosylation and increases lipid absorption in the intestine, was measured at the time of fasting in all model rats. The concentration of the plasma GLP-2 was significantly higher in NASH ($P < 0.01$) and NAFL models ($P < 0.05$) compared to the control (Fig. 5A). Next, we intraperitoneally administered GLP-2 to normal SD rats and evaluated TG concentration in the portal vein. TG concentration in the portal vein was significantly increased in the GLP-2 administration group ($P < 0.01$; Fig. 5B).

An increase in trans-portal PA activates HSC

We injected PA into the liver of normal SD rats via the portal vein and assessed the expression of genes related to HSC activation (Fig. 6A). Administration of PA significantly increased *Col1A1, Acta2, Tgfb, Timp*, and *Pai1* mRNA levels in the liver ($P < 0.01$). Furthermore, PA administration increased the expression of α-SMA in the liver (Fig. 6B).

Discussion

This study was designed to evaluate the absorption kinetics of PAs in the intestine and evaluate the effect of PAs, via the portal vein, on the activation of HSCs in NASH. We found that the relative PA change after meals was significantly increased in NASH patients compared to controls. PA concentration in the portal vein in NASH model rats was increased after meals due to the upregulation of genes related to intestinal PA absorption and CM formation. Furthermore, we showed that the influx of PA to the liver activated HSCs involved in liver fibrosis. This is the first study, to our knowledge, to report that increased intestinal PA absorption affects liver fibrosis in NASH.

Dietary LCFAs are resynthesized into TGs at the ER of intestinal cells and incorporated into CMs[19,20]. The present study showed that the number of CM particles and CM-TG concentrations in blood were higher in NASH rats than in control and NAFL rats. Furthermore, the portal PA level was higher in the NASH group than in the control and NAFL groups. These results revealed increased intestinal PA absorption in NASH, suggesting that increased intestinal absorption increased PA flow to the liver in NASH.

Next, the expression of factors involved in FA absorption (CD36, APOB, L-FABP, and I-FABP), as well as factors involved in CM synthesis (MTP and FATP4), were significantly higher in the jejunum of NASH rats than in that of control and NAFL rats. In NASH rats, glycosylated CD36 protein was also significantly higher. Highly glycosylated CD36 is expressed in the apical membrane of enterocytes[21], and CD36 is known to be involved in the absorption of LCFAs and the formation and secretion of intestinal CMs[22-25]. Our data suggest that CD36, upregulated in the intestine of NASH rats, may increase the absorption of PAs from the intestine.

Furthermore, we confirmed that plasma GLP-2 concentrations were increased in the NASH group. GLP-2 activates intestinal CD36 by glycosylation and increases FA absorption and CM synthesis in the intestine[26,27]. This result supported that PA absorption and upregulated CD36 expression were increased in the intestine of NASH rats.

Interestingly, the expression of MTP and APOA-IV was significantly increased in the jejunum of NASH rats. MTP regulates CM synthesis, and CM-mediated FA secretion is highly dependent on MTP[23]. APOA-IV is involved in the uptake of TGs into the CM[28] and upregulates MTP mRNA and protein expression[29]. APOA-IV in the intestine is upregulated by the absorption of dietary LCFAs[24,30]. These results suggest that increased PA absorption might induce higher MTP expression via APOA-IV overexpression in NASH.

This study showed that PA administration via the portal vein to the liver increased the mRNA levels of molecules involved in HSCs activation. Absorbed LCFA in the intestine generally flows into the liver via the portal vein as a component of CM[31]. PA has been reported to activate HSCs[32]. Activated HSCs are known to enhance the expression of TGF-β, COL1A1, α-SMA, TIMP, and PAI-1, which are involved in liver fibrosis[33-38]. Previous studies have shown that blood PA concentrations in cirrhotic patients are associated with the degree of liver fibrosis and that PA concentrations were high even before the onset of cirrhosis[39,40]. We showed that intestinal PA absorption and PA concentration in portal blood were increased in NASH rats. Our results suggest that the influx of PAs into the liver may activate HSCs and affect liver fibrosis progression.

Certain limitations were noted in the current study. Although we demonstrated that increased intestinal PA absorption caused hepatic HSC activation in NASH rats, we are unsure whether the same phenomenon occurs in humans.

In conclusion, PA absorption increases in the jejunum of NASH rats due to the upregulation of intestinal glycosylated CD36 and MTP (Fig. 7). Furthermore, increased PA influx into the liver due to high intestinal PA absorption may activate HSCs and affect the development of liver fibrosis. Inhibition of the protein associated with intestinal PA absorption may prevent HSC activation and liver fibrosis in NASH.

Declarations

Acknowledgments

We thank Takana Fujino, Chie Takeichi, Kenji Tanimoto, and Ayumi Sumizaki for their technical assistance.

Financial support: This work was partially supported by JSPS (Japan Society for the Promotion of Science) KAKENHI Grant Number JP17K15951 to H.U. and JSPS KAKENHI Grant Number JP18K08007 to Y.H.

Author contributions

Conceptualization and formal analysis, funding acquisition, investigation, methodology, resources, software, validation, visualization: M.H., Y.Y., H.U., Y.H.; data curation: M.H, Y.Y., O.Y., L.S., M.M., B.M., E.T., Y.I.; supervision: Y.H.; writing – original draft: M.H., Y.Y., H.U., E.T., Y.I., Y.H.; writing – review and editing; O.Y., L.S., M.M., B.M., Y.H. All the authors approved the final draft of the submitted manuscript.

Competing interest statement

The authors declare no conflicts of interest regarding this article.

Data availability statement

The datasets generated during and/or analyzed during the current study are available from the corresponding author on reasonable request.

References

1. Naga, C. *et al*. The diagnosis and management of nonalcoholic fatty liver disease: Practice guidance from the American Association for the Study of Liver Diseases. *Hepatology* **67**, 328–357 (2018).
2. Feldstein, AE. *et al*. Free fatty acids promote hepatic lipotoxicity by stimulating TNF-alpha expression via a lysosomal pathway. *Hepatology* **40**, 185-194 (2004).
3. Joshi-Barve, S. *et al*. Palmitic acid induces production of proinflammatory cytokine interleukin-8 from hepatocytes. *Hepatology* **46**, 823-830 (2007).
4. Hirsova, P. Ibrahim, SH. Gores, GJ. & Malhi, H. Lipotoxic lethal and sublethal stress signaling in hepatocytes: relevance to NASH pathogenesis. *J Lipid Res* **57**, 1758-1770 (2016).
5. Ralston, JC. Lyons, CL. Kennedy, EB. Kirwan, AM. & Roche, HM. Fatty acids and NLRP3 inflammasome-mediated inflammation in metabolic tissues. *Annu Rev Nutr* **37**, 77-102 (2017).
6. Postic, C. & Girard, J. Contribution of de novo fatty acid synthesis to hepatic steatosis and insulin resistance: lessons from genetically engineered mice. *J Clin Invest* **118**, 829-838 (2008;).
7. Donnelly, KL. *et al*. Sources of fatty acids stored in liver and secreted via lipoproteins in patients with nonalcoholic fatty liver disease. *J Clin Invest* **115**, 1343-1351 (2005).
8. Utsunomiya, H**.** *et al*. Upregulated absorption of dietary palmitic acids with changes in intestinal transporters in non-alcoholic steatohepatitis (NASH). *J Gastroenterol* **52**, 940–954 (2017).
9. Cabré, E. *et al*. Absorption and transport of dietary long-chain fatty acids in cirrhosis: a stable-isotope-tracing study. *Am J Clin Nutr* **81**, 692-701 (2005).
10. Tsuchida, T. & Friedman, SL. Mechanisms of hepatic stellate cell activation. *Nat Rev Gastroenterol Hepatol* **14**, 397-411 (2017).
11. Abumrad, NA. el-Maghrabi, MR. Amri, EZ. Lopez, E. & Grimaldi, PA. Cloning of a rat adipocyte membrane protein implicated in binding or transport of long-chain fatty acids that is induced during preadipocyte differentiation. Homology with human CD36. *J Biol Chem* **268**, 17665–17668 (1993).
12. Siddiqi, S. Sheth, A. Patel, F. Barnes, M. & Mansbach, . CM. Intestinal caveolin-1 is important for dietary fatty acid absorption. *Biochim Biophys Acta* **1831**, 1311–21 (2013).
13. Hussain, MM. A proposed model for the assembly of chylomicrons. *Atherosclerosis* **148**, 1–15 (2000).

14. Milger, K. *et a* Cellular uptake of fatty acids driven by the ER-localized acyl-CoA synthetase FATP4. *J Cell Sci* **119**, 4678-4688 (2006).
15. Alpers, DH. Strauss, AW. Ockner, RK. Bass, NM. & Gordon, JI. Cloning of a cDNA encoding rat intestinal fatty acid binding protein. *Proc Natl Acad Sci USA* **81**, 313–317 (1984).
16. Gordon, JI. Alpers, DH. Ockner, RK. & Strauss, AW. The nucleotide sequence of rat liver fatty acid binding protein mRNA. *J Biol Chem* **258**, 3356–3363 (1983).
17. Iqbal, J. *et al*. IRE1beta inhibits chylomicron production by selectively degrading MTP mRNA. *Cell Metab* **7**, 445–455 (2008).
18. Levy, E. et al. Expression of Sar1b enhances chylomicron assembly and key components of the coat protein complex II system driving vesicle budding. *Arterioscler Thromb Vasc Biol* **31**, 2692–2699 (2011).
19. Pepino, MY. Kuda, O. Samovski, D. & Abumrad, NA. Structure-function of CD36 and importance of fatty acid signal transduction in fat metabolism. *Annu Rev Nutr* **34**, 281-303 (2014).
20. Abumrad, NA. & Davidson, NO. Role of the gut in lipid homeostasis. *Physiol Rev* **92**, 1061-1085 (2012).
21. Rocca, AS. LaGreca, J. Kalitsky, J. & Brubaker, PL. Monounsaturated fatty acid diets improve glycemic tolerance through increased secretion of glucagon-like peptide-1. *Endocrinology* **142**, 1148-1155 (2001).
22. Drover, VA. *et al*. CD36 deficiency impairs intestinal lipid secretion and clearance of chylomicrons from the blood. *J Clin Invest* **115**, 1290-1297 (2005).
23. Nauli, AM. *et al*. CD36 is important for chylomicron formation and secretion and may mediate cholesterol uptake in the proximal intestine. *Gastroenterology* **131**, 1197-1207 (2006).
24. Nassir, F. Wilson, B. Han, X. Gross, RW. & Abumrad, NA. CD36 is important for fatty acid and cholesterol uptake by the proximal but not distal intestine. *J Biol Chem* **282**, 19493-1501 (2007).
25. Hussain, MM. Intestinal lipid absorption and lipoprotein formation. *Curr Opin Lipidol* **25**, 200-206 (2014).
26. Hsieh, J. *et al*. Glucagon-like peptide-2 increases intestinal lipid absorption and chylomicron production via CD36. *Gastroenterology* **137**, 997–1005 (2009).
27. Brubaker, PL. Izzo, A. Hill, M. & Drucker, DJ. Intestinal function in mice with small bowel growth induced by glucagon-like peptide-2. *Am J Physiol* **272**, E1050-E1058 (1997).
28. Lu, S. *et al*. Overexpression of apolipoprotein A-IV enhances lipid secretion in IPEC-1 cells by increasing chylomicron size. *J Biol Chem* **281**, 3473-3483 (2006).
29. Yao, Y. *et al*. Regulation of microsomal triglyceride transfer protein by apolipoprotein A-IV in newborn swine intestinal epithelial cells. *Am J Physiol Gastrointest Liver Physiol* **300**, G357-G363 (2011).
30. Kalogeris, TJ. Monroe, F. Demichele, SJ. & Tso, P. Intestinal synthesis and lymphatic secretion of apolipoprotein A-IV vary with chain length of intestinally infused fatty acids in rats. *J Nutr* **126**, 2720-2729 (1996).

31. Farrell, JJ. Digestion and absorption of nutrients and vitamins In: Feldman M, Friedman LS, Sleisenger MH, eds. *Sleisenger & Fortrand's Gastrointestinal and Liver Disease. 9th ed.* Philadelphia, PA: WB Saunders Co, 1695–1735 (2010).
32. Imai, Y. *et al*. Stimulated hepatic stellate cell promotes progression of hepatocellular carcinoma due to protein kinase R activation. *PLoS One* **14**, e0212589 (2019).
33. Dewidar, B. Meyer, C. Dooley, S. & Meindl-Beinker, AN. TGF-β in hepatic stellate cell Activation and liver fibrogenesis-updated 2019. *Cells* **8**, E1419 (2019).
34. Tsuchida, T. & Friedman, SL. Mechanisms of hepatic stellate cell activation. *Nat Rev Gastroenterol Hepatol* **7**, 397-411 (2017).
35. Henderson, NC. *et al*. Targeting of αv integrin identifies a core molecular pathway that regulates fibrosis in several organs. *Nat Med* **19**, 1617-1624 (2013).
36. Iredale, JP. Thompson, A. & Henderson, NC. Extracellular matrix degradation in liver fibrosis: Biochemistry and regulation. *Biochim Biophys Acta* **1832**, 876-883 (2013).
37. Sookoian, S. *et al*. Circulating levels and hepatic expression of molecular mediators of atherosclerosis in nonalcoholic fatty liver disease. *Atherosclerosis* **209**, 585-591 (2010).
38. Moreira, RK. Hepatic stellate cells and liver fibrosis. *Arch Pathol Lab Med* **131**, 1728-1734 (2007).
39. Arain, SQ. Talpur, FN. Channa, NA. Ali, MS. & Afridi, HI. Serum lipid profile as a marker of liver impairment in hepatitis B Cirrhosis patients. *Lipids Health Dis*. **16**, 51 (2017).
40. Yoo, HJ. *et al*. Liver cirrhosis patients who had normal liver function before liver cirrhosis development have the altered metabolic profiles before the disease occurrence compared to healthy controls. *Front Physiol*. **10**, 1421 (2019).
41. Ichimura, M. *et al*. A diet-induced Sprague-Dawley rat model of nonalcoholic steatohepatitis-related cirrhosis. *J Nutr Biochem* **40**, 62-69 (2017).
42. Bligh, EG. & Dyer, WJ. A rapid method of total lipid extraction and purification. *Can J Biochem Physiol* **37**, 911-917 (1959).
43. Rivero-Gutierrez, B. Anzola, A. Martine-Augustin, O. Medina, FS. Stain-free detection as loading control alternative to ponceau and housekeeping protein immunodetection in western blotting. *Anal Biochem* **467**, 1-3 (2014).

Figures

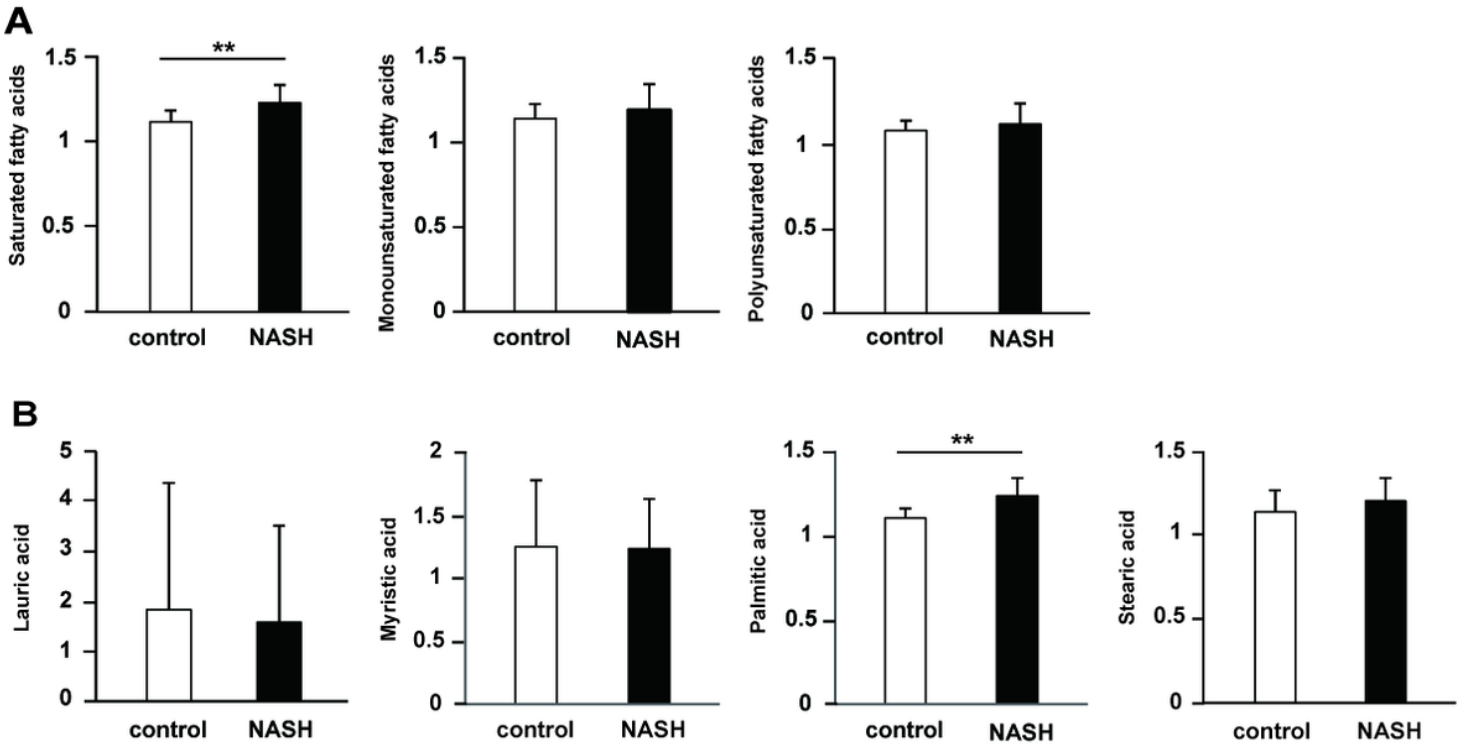

Figure 1

Relative change in fatty acids in human NASH patients (N=41) and control patients (N=39). (A) Relative change in saturated fatty acids (SFA), monounsaturated fatty acids, and polyunsaturated fatty acids. **P < 0.01. (B) Relative change in lauric, myristic, palmitic, and stearic acid in the fraction of SFAs. **P < 0.01.

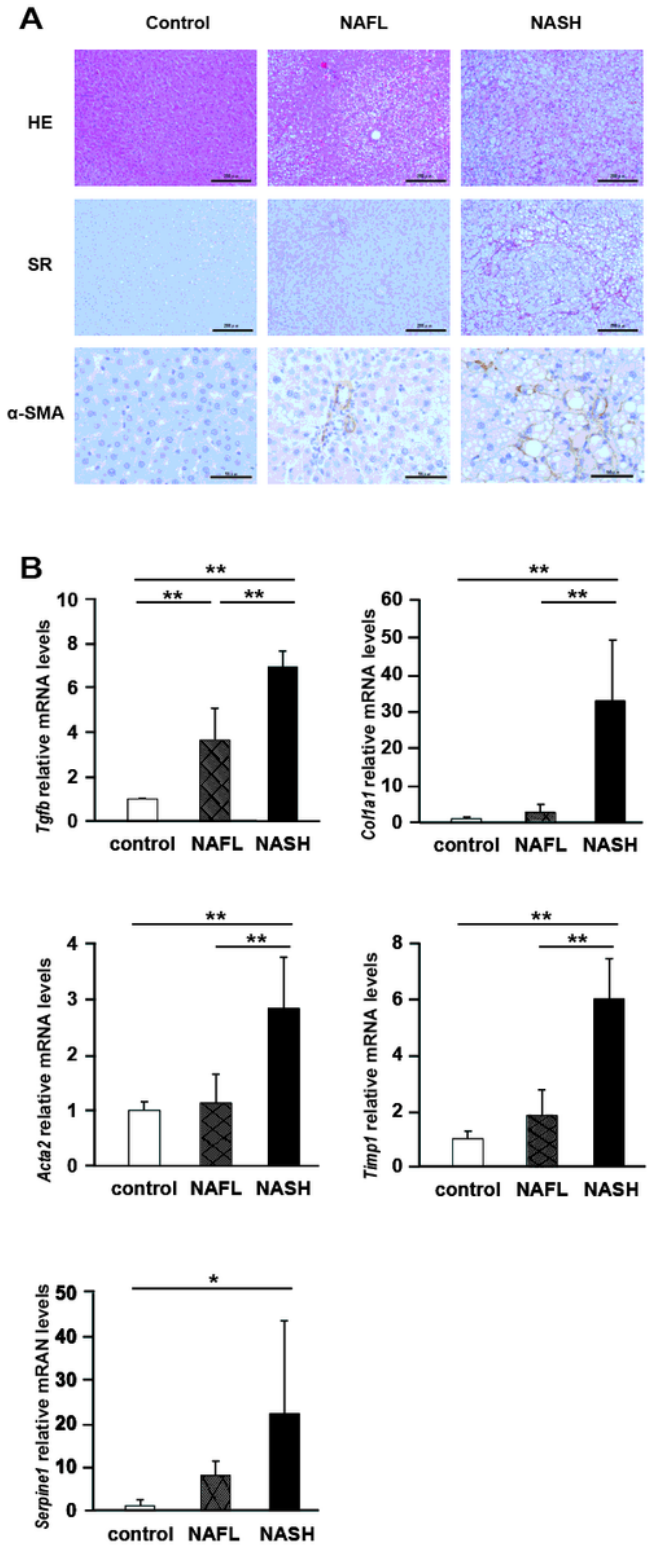

Figure 2

Liver fibrosis and HSC activation in NASH rats. (A) Representative images of liver sections stained with hematoxylin and eosin (H&E) stain, Sirius Red stain, and anti-α-SMA antibody. (B) The mRNA levels of the following factors were related to liver fibrosis: Transforming growth factor-β (Tgfb), collagen 1a1 (Col1a1), α-smooth muscle actin (Acta2), tissue inhibitor of metalloproteinase 1 (Timp1), and plasminogen activator inhibitor 1 (Serpine1). N = 5 per group. *P < 0.05, **P < 0.01.

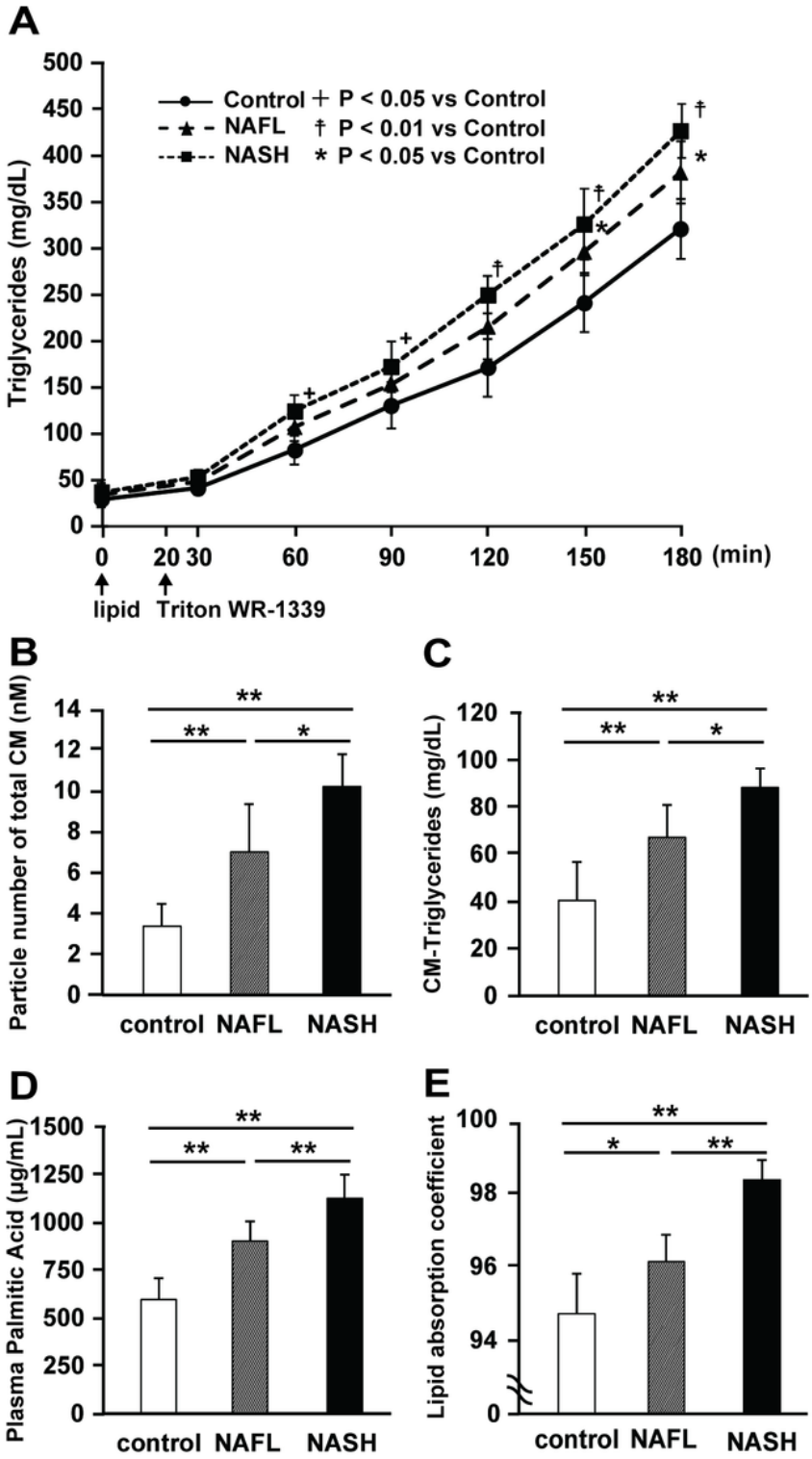

Figure 3

Lipid and fatty acid absorption increased in the intestine of NASH rats. (A) Time-dependent increase in triglyceride (TG) level in the plasma of each model rat provided by lipid emulsion and Triton infusion (N = 6 per group; P < 0.05, NASH vs. control; *P < 0.05, NAFL vs. control; P < 0.01, NASH vs. control). (B) Changes in total chylomicron (CM) particle number in portal blood measured using HPLC before and 180 min after lipid administration (N = 6 per group; *P < 0.05; **P < 0.01). (C) Changes in chylomicron TG (CM-

TG) concentration in portal vein blood measured using HPLC before and 180 min after lipid administration (N = 6 per group; *P < 0.05; **P < 0.01). (D) Changes in palmitic acid concentration in portal vein blood measured using gas chromatography before and 180 min after lipid administration (N = 6 per group; **P < 0.01). (E) Lipid absorption coefficient (LAC) in each group. LAC was measured when the same diet (MFD) was ingested (N = 6 per group; *P < 0.05, **P < 0.01).

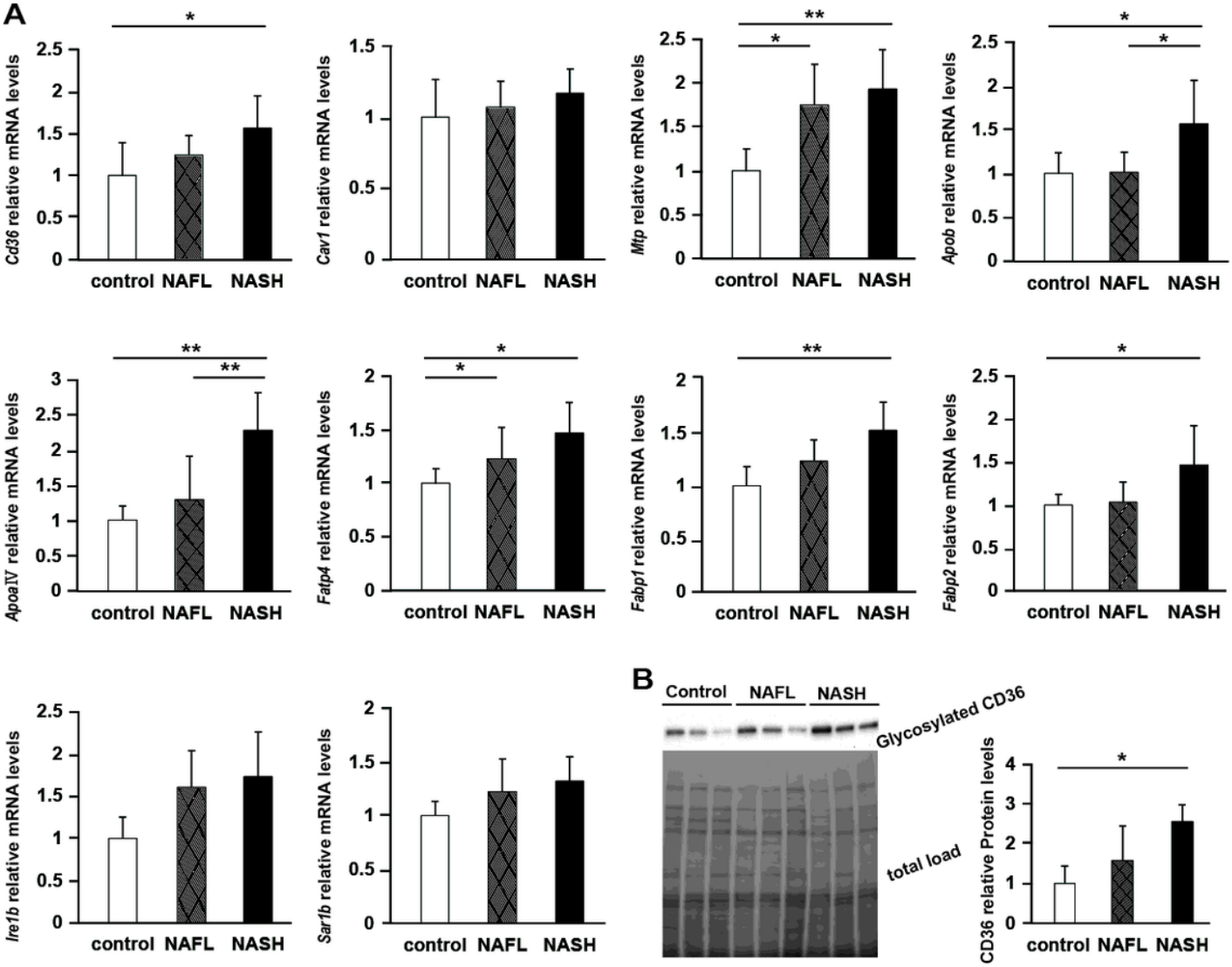

Figure 4

Expression of genes and proteins involved in fatty acid and lipid absorption in the intestine. (A) The mRNA levels of the following genes were related to the transport of long-chain fatty acids and lipids. Cluster of differentiation (Cd36), caveolin 1 (Cav1), microsomal triglyceride transfer protein (Mtp), apolipoprotein B (Apob), apolipoprotein A-IV (ApoaIV), fatty acid transporter protein 4 (Fatp4), fatty acid-binding protein (Fabp), including liver FABP (Fabp1) and intestinal FABP (Fabp2), inositol-requiring enzyme1b (Ire1b), and secretion associated, Ras-related GTPase1b (Sar1b). N = 6 per group. *P < 0.05, **P < 0.01. (B) Western blot analysis of glycosylated CD36 protein in jejunal tissue. N = 3 per group. *P < 0.05.

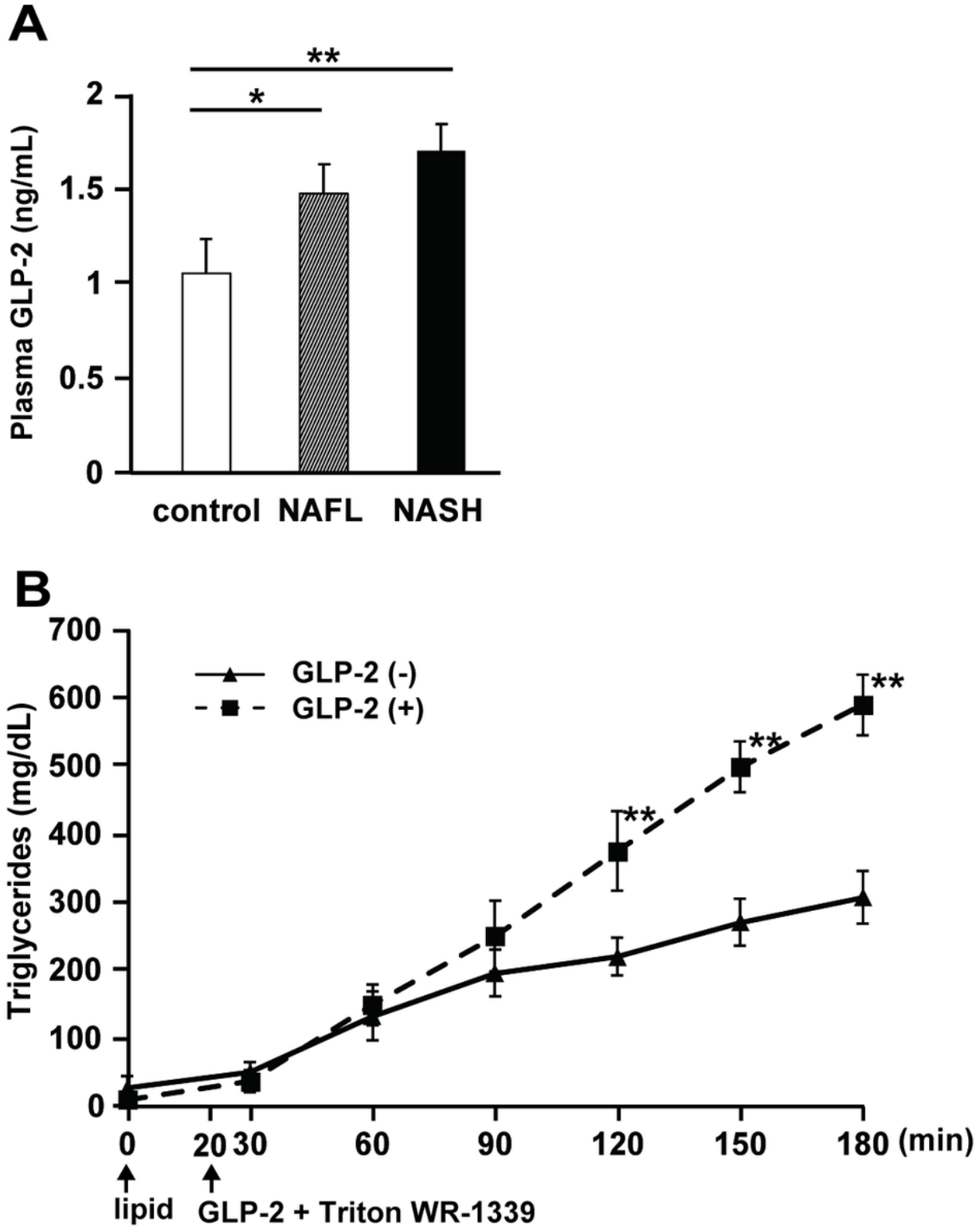

Figure 5

Promotion of intestinal lipid absorption by glucagon-like peptide-2 (GLP-2). (A) Fasting blood GLP-2 levels in each group (N = 5 per group; *P < 0.05, **P < 0.01). (B) Time-dependent increase in plasma triglyceride (TG) level in each model rat administered lipid emulsion and Triton infusion, as required. GLP-2 was administered 20 min after the administration of the lipid emulsion. N = 6 per group. **P < 0.01.

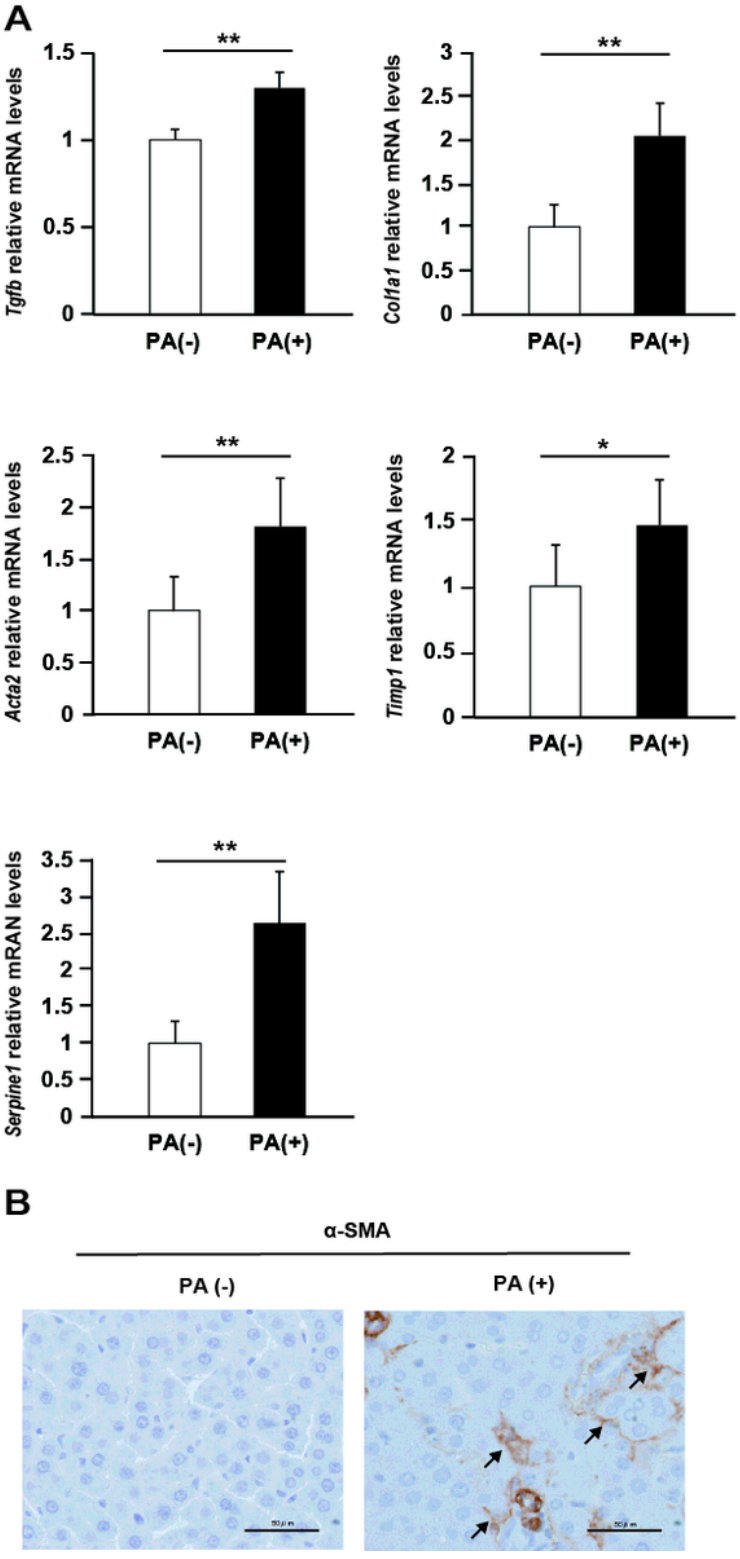

Figure 6

HSC activation using palmitic acid. (A) The mRNA levels of the following genes were related to liver fibrosis. Transforming growth factor-β (Tgfb), collagen 1a1 (Col1a1), α-smooth muscle actin (Acta2), tissue inhibitor of metalloproteinase 1 (Timp1), and plasminogen activator inhibitor 1 (Serpine1). N = 6 per group; *P < 0.05. **P < 0.01. (B) Immunohistochemistry of α-SMA expression in rat liver using anti-α-SMA antibody.

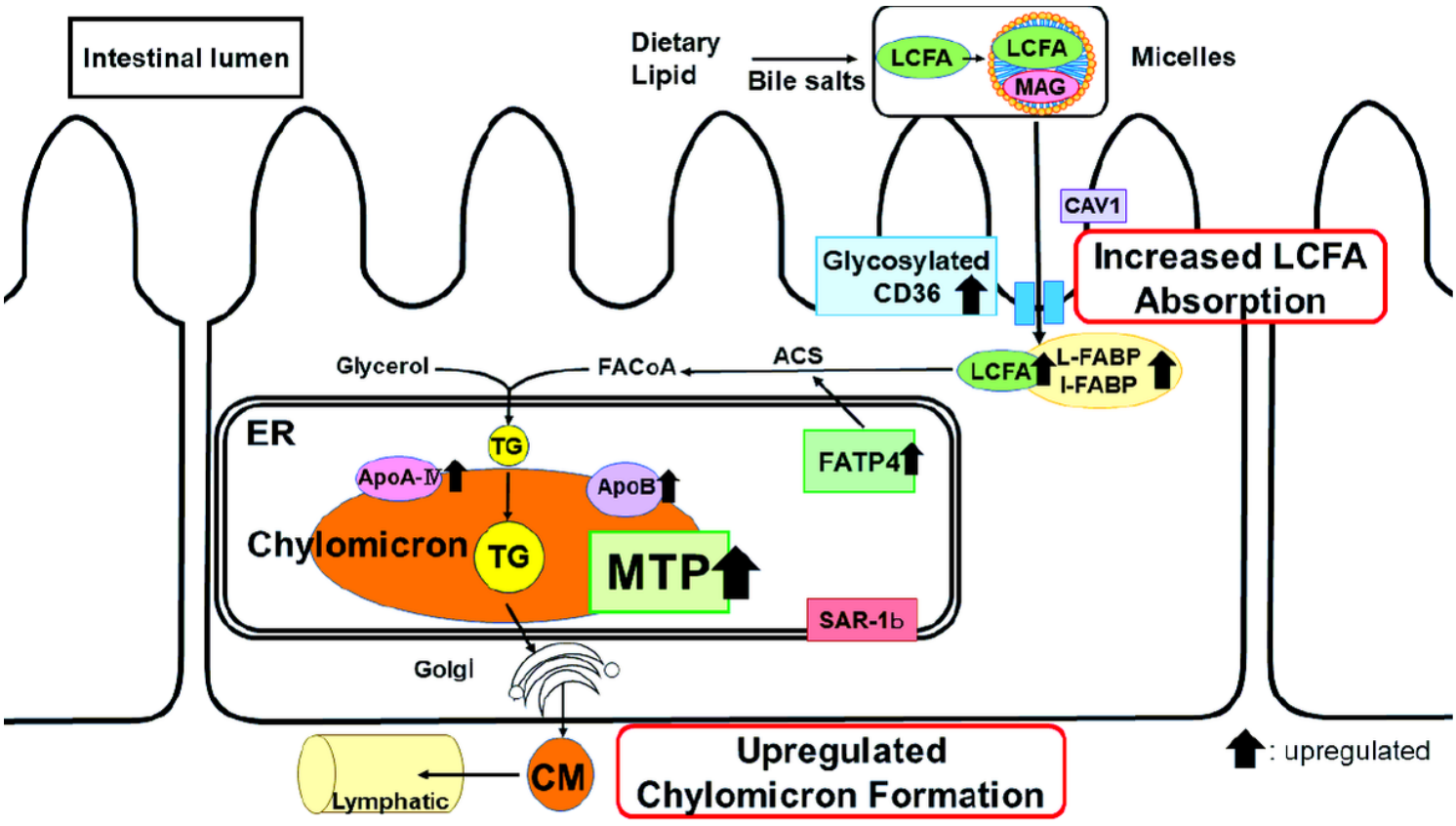

Figure 7

Model of lipid and fatty acid (FA) absorption in NASH. First, the expression of CD36 was enhanced in intestinal villi, followed by an increase in FA uptake into intestinal cells. Second, triglycerides (TG) were synthesized from long-chain fatty acids, which were incorporated into chylomicrons in the endoplasmic reticulum (ER) via microsomal triglyceride transfer protein (MTP). Third, the synthesized chylomicron was secreted from the ER and flowed into the lymphatic vessels via the Golgi apparatus. LCFA, Long-chain fatty acid; ACS, acyl-CoA synthetase; FA-CoA, fatty acyl-CoA;

Supplementary Files

This is a list of supplementary files associated with this preprint. Click to download.

- supplementaryinformation.docx